Reliability of III-V/Si heterogeneously integrated lasers

Felipe Vallini*[a], Karthik Narayanan[a], Christopher Helms[b], Wendai Wang[c], George Ghiurcan[d], Pierre Doussiere[e], Richard Jones[e], Isako Hoshino[c], Quan Tran[c] and Kishore Kamath[e]
[a]Foundry Quality and Reliability, Intel Corporation, Hillsboro, OR USA 97124; [b]Foundry Quality and Reliability, Intel Corporation, Rio Rancho, NM USA 87124; [c]Foundry Quality and Reliability, Intel Corporation, Santa Clara, CA USA 95054; [d]Silicon Photonics Process Development and Manufacturing, Intel Corporation, Rio Rancho, NM USA 87124; [e]Integrated Photonic Solutions, Intel Corporation, Santa Clara, CA USA 95054

ABSTRACT

Intel's integrated InP-based hybrid laser technology is emerging as a promising option for co-packaged optics due to its inherent elimination of several failure modes of conventional discrete distributed feedback lasers, namely, (1) lack of catastrophic optical mirror damage due to no exposed III-V facets, (2) reduced epitaxial interface defects due to no III-V re-growth steps, and (3) no electrostatic discharge failures during handling and assembly. For elimination of other failure modes due to crystalline defects such as dark line dislocations and catastrophic optical bulk damage, the approach of testing every laser using a wafer-scale, high-volume manufacturing burn-in test system to screen out early life failures prior to field deployment has been proven effective. Specifically, the reliability of Intel's lasers is demonstrated with 45,000 hours of high temperature operating life testing on 32 units with negligible observed degradation. A failure rate in time of < 0.1 FIT is demonstrated with accelerated life testing of over 55 thousand lasers and validated as 0.05 FIT by analyzing field deployment data collected from more than 6 million hybrid lasers with 100% Failure Analysis (FA) confirmation over a period of 3 years.

Keywords: Heterogeneously integrated lasers, reliability, semiconductor laser, photonics integrated circuits, silicon photonics

1. INTRODUCTION

Silicon photonics has become a high volume, commercially available technology, essential for optical communications and interconnects due to its high-speed and high-bandwidth data transfer rates at long distances in comparison with electronic links that are limited to <10m for signals modulated above 100Gbps and beyond [1]. The deployment of millions of silicon photonics transceivers by Intel and other companies over the last decade has become essential to meet the ever-growing demand of global data traffic, and support Datacenter speed and performance scaling. This demand has further escalated with the explosion in the field of artificial intelligence (AI), particularly in data-intensive tasks requiring AI clusters, composable accelerators, distributed computing and memory disaggregation [2]. These new tasks demand a significant increase in interconnect bandwidth while reducing power consumption due to the number of FLOPs required to train AI models [3,4]. Such requirements can only be enabled by custom hardware and architectures, which require new and reliable high-speed and high-bandwidth solutions, bringing optics in closer proximity to compute dies and switch ASICs, through Co-Packaged Optics (CPO).

CPO consist of a system on chip (e.g. XPU) connected through a substrate with an Optical Compute Interconnect (OCI) chiplet for electrical to optical data conversion. The OCI consists of a Photonic Integrated Circuit (PIC) flip-chip bonded to an Electronic Integrated Circuit (EIC), each from different process nodes so their individual and overall performance can be optimized [5]. Although the solution is promising to solve the bandwidth and power bottleneck, reliability concerns due to the system's complexity comprising of the XPUs, substrate interconnects, OCI die-stack, individual EIC and PIC itself have been raised. The focus of this article is on the reliability of PICs used for CPO, more precisely on the reliability of integrated semiconductor lasers used as sources in such PICs. Any laser failure on a PIC can lead to significant data transmission errors, network disruption and system down times, resulting in high maintenance cost, while modules/systems become more expensive if redundant lasers are included to mitigate the risks. The disruption and cost increase significantly when PICs are part of a CPO architecture without front-plane swappable transceivers.

*felipe.vallini@intel.com

Silicon Photonics XX, edited by Graham T. Reed, Jonathan Bradley,
Proc. of SPIE Vol. 13371, 1337106 · © 2025 SPIE
0277-786X · doi: 10.1117/12.3043449

As a reference, consider conventional 800G optical transceiver modules, whose failure in time (FIT) is reported to be up to ~200 (1 FIT is defined as 1 failure in 1 billion device hours), where 90% of the failures are due to lasers [6]. In this case, there would be roughly one 800G module failure every two days for 100,000 modules deployed in a data center. Such failure rate is worrisome as the number of lasers in a PIC for Optical I/O applications is expected to be many more than of commercial transceivers. Therefore, for CPO to be considered a reasonable solution, its lasers, external or integrated, needs to meet the reliability requirement of less than 2 FIT to reduce network downtime and to lower the cost of serviceability.

In this article, common InP-based semiconductor lasers failure modes and root cause are reviewed in section II, focusing on distributed feedback (DFB) lasers, electroabsorption modulated lasers (EMLs) or directly modulated lasers, as examples. We discuss how Intel's heterogeneously integrated laser architecture inherently mitigates most of these failure modes besides Dark Line Dislocations (DLDs) and Catastrophic Optical Bulk Damage (COBD). These last two failure modes are mitigated by using a wafer-scale screening platform which will be discussed in Section III. In section IV, an acceleration model to estimate the escape defective parts per million (DPPM) is proposed and experimentally validated with field return data, showing outstanding reliability results of < 0.1 FIT. Section V concludes the article summarizing the excellent reliability of heterogeneously integrated lasers.

2. COMMON FAILURE MODES ON CONVENTIONAL VS. HETEROGENOUS LASERS

In this section, common failure models of conventional semiconductor lasers will be compared with heterogeneously integrated lasers, with both laser types illustrated in Figure 1. For conventional lasers, InP-based DFBs and EMLs are considered. These traditional lasers require epitaxy re-growth to create optical/electrical confinement (regrown layers shown in Figure 1(a)) and die singulation to create the laser facet and enable light coupling from the laser source to an optical fiber or PIC [7]. The active region in Figure 1(a) may have an in-plane grating structure that would also require an extra re-growth step. For use with silicon photonics this laser can be an external source to a PIC or bonded onto the PIC. For heterogeneously integrated lasers, also called hybrid lasers, a singulated III-V epitaxy die is bonded to a 300mm SOI wafer already processed with Si waveguides, in-plane grating structures, and all the other non InP-based components. The semiconductor laser is fabricated after the bonding step, followed by passivation, metallization and annealing processes [8]. In this case, no re-growth is utilized and there are no III-V facets since the light is coupled directly into the silicon waveguide.

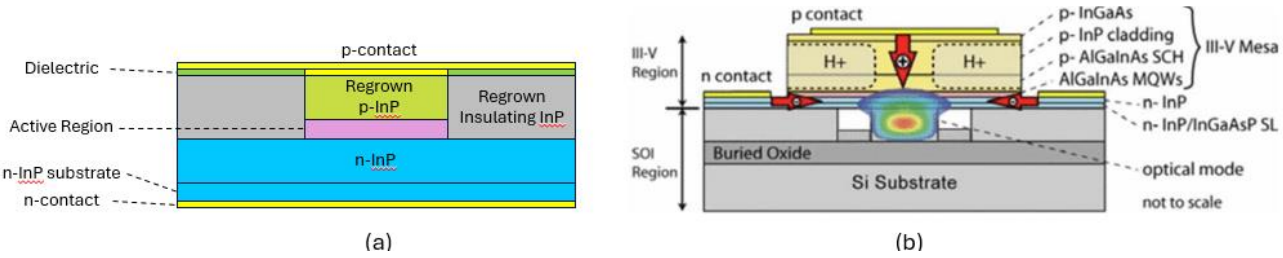


Figure 1. Schematics comparing (a) a conventional DFB laser containing multiple re-growth steps to create a grating into the MQW region and a current confinement channel around it, with (b) Intel Silicon Photonics heterogeneously integrated laser, where the grating is etched on the Si waveguide prior to bonding of the III-V epitaxial stack and a current channel created by H^+ implants into the p-InP layer. Dimensions are not to scale, and designs can have p and n layers swapped.

A semiconductor laser, conventional or heterogeneously integrated, can operate at two different conditions: constant output optical power or constant bias current, depending on the system application. A failure is defined when the laser bias current at a fixed output optical power increase above certain value, or analogously, when the output optical power at a fixed bias current drops below certain value. The laser output optical power and the bias current are coupled through the laser rate equations [7], meaning that the failure of one of them, usually leads to a failure for the other, however the root cause can be significantly different depending on the failure mode observed. From a field deployment perspective, these failures can be categorized as early-life, wearout, or random failures depending on when they occur during the lifetime of a component, as depicted in Figure 2. Wearout are intrinsic failures observed close to, or after the expected lifetime for the laser, while early-life failures are mostly due to extrinsic defects and observed at the first years of operation. Early-life failures can be reduced with production burn-in screening, properly designed to ensure the "weakest" parts are not deployed, reducing the

failure rate for the first years of operation. Random failures are observed in between early-life and wearout failures and can be due to un-optimized epitaxy growth, poor extrinsic defects screening, device design flaws and ESD events.

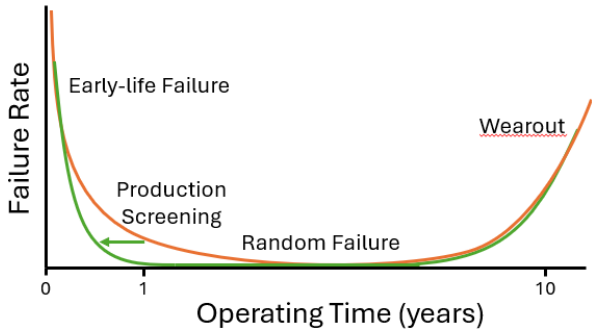


Figure 2. Typical failure rate vs. operating time curve (bathtub curve) illustrating the three regimes of failures: early life, wearout and random failures. The green curve illustrates the reduction on the early-life failure rate if proper production screening is utilized to burn-in the "weakest" parts prior to field deployment.

Some of the traditional failure modes for conventional semiconductor lasers that are considered for the comparison in this article are: sudden stop of lasing due to Electrostatic Discharge (ESD); wear-out degradation, sudden degradation due to Catastrophic Optical Mirror / Bulk Damage (COMD / COBD), and DLDs. Each one of these failure mechanisms are discussed below, with a description of the reliability advantages of heterogeneously integrated lasers compared to conventional semiconductor lasers.

2.1 Random failure #1: ESD

Although this article is not intended to cover reliability issues due to packaging and assembly, an obvious advantage of an integrated laser source worth mentioning is the lack of random failures due to ESD caused in the manufacturing line and/or handling. The ESD damage occurs when an electrical device, optoelectronic in this case, receives a voltage across, current through, or power dissipated above a certain safety limit, leading to damage or malfunction and an unpredictable reduction of its lifetime. Assuming there is no design, testing, or switching (AC) operation issues on the assembly line, the root cause of ESD can be attributed to unpowered device handling such as: proximity with charged devices, boards and systems, charged personnel, field induced events and even lack of / poor grounding.

Conventional transceiver assembly relies on attaching independent chiplets or devices onto a substrate or a "gold-box", where the laser in singulated die-form is more susceptible to ESD events. Having the laser source integrated on the PIC prevents any potential ESD/EOS concern during assembly. A comparison schematic is shown in Figure 3. The laser area within a PIC is just a small portion of the full die, sometimes surrounded by other components, which improves the shielding from ESD. The heterogenous PIC architecture contains multiple and distributed electrical pathways improving the dissipation of charges induced by ESD, also reducing the risk of failure due to a single-point ESD event. Lastly, the Silicon-on-Insulator wafer used has better thermal conductivity than InP, improving heat dissipation and reducing the localized heating from an ESD event that could trigger a thermal runaway effect on the III-V laser.

To demonstrate the robustness of hybrid lasers to ESD, we submitted tens of PICs to Human Body Model (HBM) and Charge Device Model (CDM) stress following the guidelines from the standards JS-001-2012 and JESD22-C101E [9,10]. HBM testing simulates the discharge from a human body while CDM emulates charging by triboelectric effect or electrostatic induction. During the deployment of multiple generations of transceivers, hundreds of units have been submitted to both tests. Overall, Intel's hybrid lasers exhibited first observed failure at voltages above 1000V during HBM testing and above 2000V during CDM testing, far exceeding the standardized criteria of zero fail on HBM up to 150V and on CDM up to 250V.

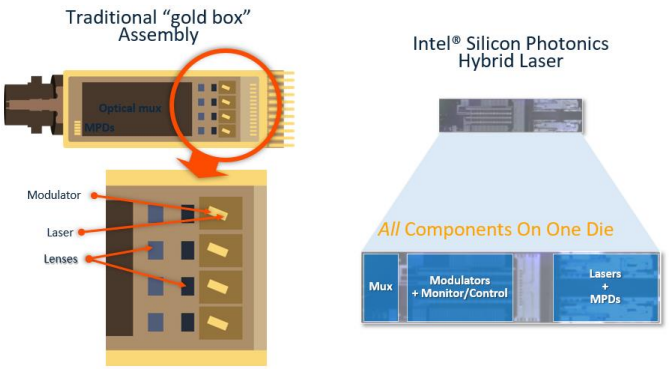


Figure 3. Schematic comparing a traditional assembled transceiver with Intel Silicon Photonics heterogeneously integrated laser.

2.2 Random and wearout failure #2: regrowth interface

Wear-out is observed through a slow degradation of the laser slope efficiency and/or a slow increase of the laser threshold current over time. The laser threshold is proportional to the threshold carrier density and reciprocal to the injected carrier lifetime. Assuming a nearly constant threshold carrier density due to carrier clamping above threshold, any degradation can be due to a reduction of the injected carrier lifetime, or more precisely, a reduction in the nonradiative recombination lifetime associated with an increase in the defect density [11]. The root cause can be related to point defect migration and the climb of dislocations close to or in the active region of the laser [12]. This migration of defects can be enhanced by the internal mechanical stress that is dependent on temperature, and noting that the dislocation propagation speed increases significantly when current is applied through the current injection channel of the laser [13]. Gradual degradation is mitigated by reducing deep-level defect centers and interface defects, with high-quality InP substrates and epitaxial growth, preventing the diffusion of metals from the ohmic contact alloys and with proper strained quantum well epitaxy engineering [14].

Conventional DFB and EMLs require at least a two-step epitaxial growth to create the buried heterostructures for electrical confinement and a grating structure for optical feedback. During the second step, called re-growth, the alloys and epitaxy heterointerfaces are prone to the creation of interface imperfections and defect states, increasing the defect density and consequently the nonradiative recombination rate, becoming more susceptible to wear out and random degradation. Intel's hybrid lasers are Al-based MQWs, MOCVD grown on InP substrates, without any re-growth step. The grating is etched into the Si waveguide prior to III-V material bonding and laser processing, while the current channel is created through proton implantation on the p-doped InP mesa during laser processing, as illustrated in Figure 1(b). The resilience of heterogeneously integrated lasers to wearout is demonstrated by High-Temperature Operating Life Testing (HTOL) following the TELCORDIA standard guidelines [15]. The HTOL stress is set at the maximum operating temperature and bias current conditions defined in each product specification and application case, and the laser performance is monitored over time. Figure 4 contains the laser bias current drift at a fixed output power normalized to the performance at time zero during a HTOL stress for 100G PSM4 (32 units) in Fig. 4(a), and for 400G DR4 (14 units) in Fig. 4(b). The tests are continuously running at 80C and at the maximum bias current specified by each product requirements. The tests reached more than 45,000 hours (PSM4) and 15,000 hours (DR4) without significant drift over time. The noise observed is due to testing equipment variability. The negligible drift observed on DR4 are due to constant laser design, epitaxy design and growth improvements during every transition to a new product or architecture.

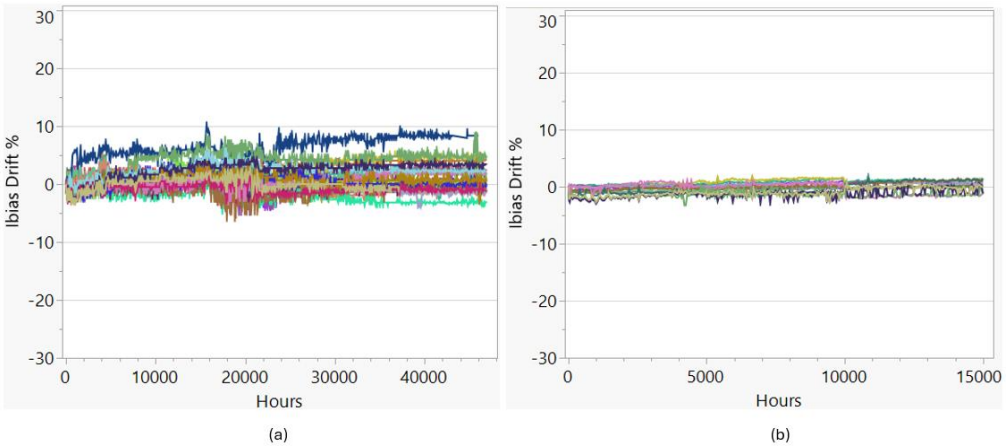


Figure 4. Normalized laser bias current versus stress hours during HTOL stress at 80C and at the maximum laser bias current specification for 32x 100G PSM4 laser units and (b) 14x 400G DR4 laser units. The tests are ongoing.

2.3 Early-life and random failure #3: COMD

In recent decades, significant advances in epitaxial growth have enabled higher quality material interfaces and reduced defect densities improving device wearout mechanisms even for epitaxy structures with multiple re-growth steps. However, conventional lasers are edge-emitting devices, and when the dies are singulated from the wafer, heterointerfaces are exposed, leading to higher surface recombination rates [16]. If the active region exposed at the facet contains Al, it is also prone to surface oxidation, leading to higher optical absorption near the cleaved facets [17]. Each factor contributes to localized light absorption spots at, or near the output facet of the laser, that produce localized heating and result in a detrimental feedback loop resulting in gradual degradation of the laser.

The described mechanism can take from ns to years to initiate, but thermomechanical gradients and stress are induced around the heating spots which can generate dislocations and their motion by recombination enhanced defect reactions (REDRs). This regime is usually reached when an optical power density COD threshold is reached, resulting in an extrinsic feedback loop called thermal runaway, where the laser facet temperatures can reach more than 1000°C and fast degradation with sudden failure of the laser is achieved [18]. This is one of the explanations for the phenomenon, but there is still debate on the field and it is not in the scope of this article to provide an in-depth description of the mechanism.

To prevent COMD, edge emitting lasers require a facet passivation step where the emitting facet is treated and/or dielectric coatings are deposited to prevent oxidation, and to reduce surface recombination velocities. With Intel's heterogeneously integrated laser, such a step is not required since the risk of COMD is nonexistent. As illustrated by Figure 5, the lasing distributed feedback mechanism is provided by gratings etched into the Si waveguide prior to bonding of the III-V epitaxy die [19]. An adiabatic taper couples the hybrid laser mode (III-V/Si) into the Si waveguide towards other components of the PIC neglecting the need for a III-V facet, and after laser fabrication the entire structure is covered with a passivation layer [20]. Heterogenous integrated lasers then inherently mitigates any potential failure due to COMD.

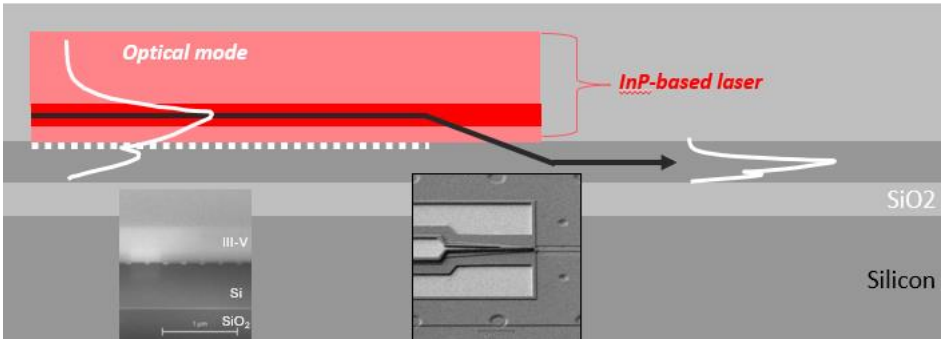


Figure 5. Schematics of a heterogeneously integrated laser and respective optical mode profile (side view). The optical mode is hybrid between the Si and the III-V layers at the DFB grating region created on Si (left inset) and an adiabatic taper (right inset) fully converts the optical mode into the PIC Si waveguide. No facets are presented.

2.4 Early-life and random failure #4: DLDs and COBD

Based on our observations, the two failure modes present in conventional lasers that are not mitigated by heterogeneously integrated lasers are those associated with DLDs and COBD. Since InGaAsP alloys properties changes more significantly at higher temperatures, Al-based MQW structures are grown to achieve higher operating optical powers at a wider and higher temperature range. Although Al-based alloys are known to be less susceptible to wear out degradation, Al-containing alloys are more susceptible to the occurrence of DLDs and more sensitive to optically activated defects that can lead to COBD.

Similar to the mechanism explained during COMD, COBD is also triggered when a thermal runaway regime is achieved, and it is related to the intracavity optical power density [21]. While COMD is triggered by facet defects, oxidation and/or surface recombination, the fast COBD phenomena requires a defect located within or close enough to the active region acting as an absorption center to trigger the degradation loop. Even with an optimized growth and fabrication process, an epitaxial interface or bulk defect may still exist and turn into a dislocation and be able to propagate from locations nearby or close to the active region. For this reason, COBD leading to sudden degradation is considered the failure mode observed while interface and bulk defects turning into DLDs are proposed as one of the main root causes.

There are multiple possible origins of DLDs, but the focus here will be two items considered relevant based on years of internal observations, divided into extrinsic and intrinsic for the sake of this discussion. Both cases are illustrated in Figure 6. Extrinsic defects here are considered, for example, as scratches on the III-V die during the die singulation or bonding process step and trapped particles at the III-V/Si bonding interface, as shown on Figure 6(a). Intrinsic defects are considered as dislocations propagating from incoming substrate defects (threading dislocations) and epitaxy grown defects such as micro twins, misfit dislocations, inclusions, stacking faults shown on Figure 6(b) and others.

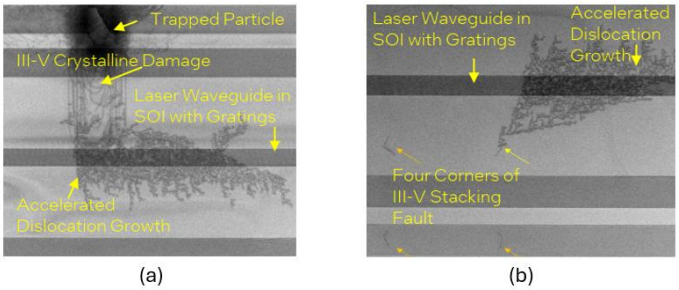


Figure 6. Examples of dislocation networks that propagated under high bias current at high temperatures originated from (a) a trapped particle at the bonding interface (extrinsic), and (b) from a stacking fault (intrinsic).

The path to eliminate the risk of COBD is then to reduce and to extinguish incoming defects, if possible. Extrinsic defects can be reduced and even eliminated through bonding process optimization and placement of proper inline defect monitoring and metrology, made possible by use of a mature 300mm CMOS factory. Intrinsic defects can be reduced through optimized epitaxy growth recipes, proper metrology monitors post epitaxy growth and stringent quality control of incoming substrates. Even with all right monitors and controls in place, an automated high-volume manufacturing (HVM) wafer level burn-in procedure provides high quality and efficient screening of lasers prior to field deployment to ensure the final product can meet the mission profile requirements and lifetime targets.

3. FULL WAFER-SCALE HIGH VOLUME MANUFACTURING BURN-IN SYSTEM

A burn-in step is required to stabilize the performance of heterogeneously integrated lasers and to screen out early life failures and potential escapes susceptible to COBD or other failure modes not eliminated or contained. The burn-in is realized in two steps, named as thermal burn-in and optical burn-in.

Once the hybrid lasers are stabilized with a thermal burn-in, an optical burn-in is performed. In this step, the hybrid lasers are stressed at bias currents up to ~20-50% of operating conditions and at temperatures lower than the max operating conditions, leading to optical output powers 2-3x larger than the nominal values. At these high optical powers, it is possible

to screen out "weak" lasers which would fail early due to defects associated with epi growth or processing, known as early-life-failures [22].

The two-step burn-in is performed on a 300mm wafer-scale high-volume manufacturing burn-in system with precise thermal and electrical control, and capability of stressing more than 20,000 lasers in parallel, as shown on figure 7. The platform is automated and able to provide electrical and optical testing. Every laser from all the wafers receives the two-steps burn-in and only known good dies are shipped to customers. Besides production wafer burn-in, such capability also enables reliability studies, with significantly larger sample sizes than conventional studies, to identify, model, reduce and eliminate low-probability failure modes.



Figure 7. HVM Burn-In System with precise thermal and electrical control capable of testing >20,000 heterogeneously integrated semiconductor lasers in parallel.

4. RELIABILITY MODEL AND FIELD VALIDATION

The HVM wafer-level burn-in capability together with thousands of heterogeneously integrated semiconductor lasers on a single wafer allow the development of a robust reliability model with unprecedent sample sizes. Traditional semiconductor laser reliability models are based on thermal, current density and photon density acceleration parameters; with the total stress acceleration factor (AF) described by:

$$AF = \left(\frac{J_{acc}}{J_{use}}\right)^{n} \left(\frac{P_{acc}}{P_{use}}\right)^{m} e^{\left[\frac{E_a}{k_B}\right]\left(\left(\frac{1}{T_{use}}\right)-\left(\frac{1}{T_{acc}}\right)\right)} \quad (1)$$

where J is the current density, P is the optical power density, k_B is the Boltzmann constant, and T is the temperature. E_a is the activation energy; n is the current density acceleration parameter and m is the optical power density acceleration parameter for an accelerated stress condition over the use case conditions [23].

After assessing the semiconductor laser failure modes that can occur at different operating conditions, a stress acceleration matrix is designed around the most relevant conditions to activate and accelerate a specific failure mode. The most common matrix utilized is a two-parameters inverse L-shape, with 3 different temperatures at the maximum bias stress condition and 3 different bias condition at the maximum stress temperature [24]. Knowing that optical power is a main parameter driving COD, the optical power density P for each combination of temperature and bias current must be considered as well, and more cells are required to model this extra parameter. Table 1 illustrates the stress matrix utilized to build this reliability model (note that P is not necessary the same for the cells).

Table 1. Three-dimensional accelerated stress matrix for BCOD reliability model considering 3 acceleration parameters: Current (I), Temperature (T) and Optical Power (P). Note that P is not necessarily the same for all cells.

Current/Temp	T1	T2	T3	T4
I1	P(I1, T1)	P(I1, T2)		P(I1, T4)
I2		P(I2, T2)	P(I2, T3)	P(I2, T4)
I3	P(I3, T1)	P(I3, T2)	P(I3, T3)	

A total of six wafers with a well-known defect density population were selected for the experiment and split into 4 different temperature stress conditions, following Table 1. The HVM wafer-level burn-in system permits the biasing of different reticles of a wafer at different setpoints, enabling more than one bias current condition per temperature on a single wafer. The choice of a bias current at a given temperature results in a different optical power. With such a stress matrix, the experiment is designed in such a way to have 2-3 variable conditions for one parameter (Temperature, Bias or Power), while the other two parameters are kept constant, this supports the validation of a reliability model.

4.1 Reliability Model

Six wafers containing ~10,000 lasers, were stressed at the conditions proposed on Table 1 for a minimum of 500 hours with intermediate readouts to measure the performance parameters of interest during device degradation. Some of the cells, at lower accelerated conditions, were stressed for more than 1000 hours. The failure criteria have been defined as a 30% increase in laser bias current to maintain a fixed output power. As an example of the experiment outcome, the results for three of the cells, at a single temperature (T1) but at three different bias currents (I3 > I2 > I1), are shown on Figure 8 (a). A lognormal distribution has been utilized since it provides the best fit to the available data with the lowest likelihood error. The data points fit well within this distribution with comparable slopes between the conditions, assuring the degradation observed is due to a single failure mode. The scales of the distributions overlap but not their locations, indicating, again, a good fit and the relevance of the acceleration parameters. There is a lower tail (early life failures) presented for bias currents I2 and I3 because the devices were not screened prior to this experiment, but their contribution for the fit lognormal distribution is negligible.

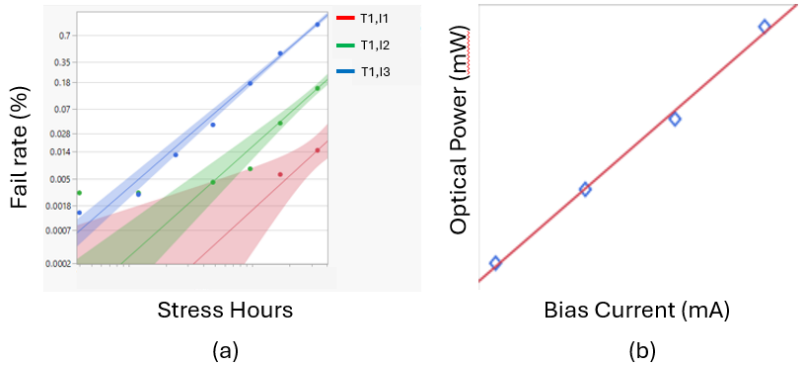


Figure 8. (a) Lognormal lifetime distribution of failures at Temperature T1 and bias currents I1, I2 and I3 (I3 > I2 > I1). (b) Linearity of laser output power versus bias current range applied during stress at a specific stress temperature.

With such a rich data set it is possible to optimize the reliability model, and evaluate different models considering a single acceleration parameter only (temperature, bias current, or optical power), two acceleration parameters (two of the single parameters together), and all three acceleration parameters. The different models were compared and a model with temperature and optical power acceleration resulted in the lowest chi-square value for an effect likelihood ratio test and reasonable physical meaning. We note that from a device perspective the optical output power vs. bias current at a fixed temperature is approximately linear, as shown in Figure 8(b), which indicates power and current are redundant parameters,

and can be used as acceleration parameters interchangeably. From a physical model standpoint, it is well known that optical power density is the fundamental parameter leading to COD [25]. For this reason, a model based on Eq. (1) with Ea and m, and n = 0 has been proposed.

Reliability data, at one of the highest acceleration cells from Table 1 (T3, I3), was collected during the qualification of Intel's FR4 (200G/400G) and DR4 (400G) pluggable transceiver modules. A total of 32 wafers from 11 different lots were tested, resulting in a total of ~55,800 lasers under stress. These wafers went through both temperature burn-in stabilization and optical burn-in screening prior to reliability testing, resulting in only 13 observable failures with COBD failure mode validated by failure analysis. The reliability model was applied to calculate the total equivalent device hours, with the use case conditions assumed to be the highest bias current specified by the product requirements, and a backside die temperature of 63C. The projected FIT rate is calculated to be 0.09 at a confidence level of 60%.

4.2 Field Return Failure Statistics

A data set from shipments to customers who participate in Intel Silicon Photonics 100% Return Material Authorization (RMA) / Failure Analysis (FA) program is compared with the FIT projections based on the proposed reliability model. The numbers of transceivers deployed on this program is 1.54 million, corresponding to 6.16 million heterogeneously integrated lasers over a period of 3 years.
Since customers don't necessarily share information regarding their actual deployment time and the allocation for utilization versus spare inventory, some assumptions are required to estimate the total equivalent device hours of operation. The first assumption is that after acquiring the parts, the deployment occurs only 1 quarter after receiving the parts. The second assumption is 75% deployment while retaining 25% of the parts as spare inventory. The sample size excludes non-laser related failures, since the focus of this article is purely laser reliability. With these assumptions and considerations, the total equivalent device hours calculated for the 6.16 million lasers shipped is ~4.15×10^{10} hours. The total number of laser failures by the time of this article is only 2, and COBD has been validated with FA. The calculated field return FIT is 0.05, a value close to the 0.09 FIT projected by the reliability model. This not only validates the model, but also confirms the impressive reliability of heterogeneously integrated lasers.

5. CONCLUSION

In this article we reviewed the most common failure modes of semiconductor lasers, highlighting how InP-based heterogeneously integrated lasers inherently eliminate most of them in comparison to conventional DFB lasers and EMLs. Such achievement is obtained by utilizing Al-based MQW material system to reduce wearout risks, removing epitaxial re-growth steps to reduce interface defect density and risk of oxidation, eliminating laser facets mitigate COMD, and preventing ESD risk since the laser is already integrated.

A mature 300mm CMOS factory and automated HVM wafer level burn-in provides high quality and efficient screening for the few failure modes still present in hybrid lasers, enabling the shipment of only "known-good-dies", where every single laser on every wafer is tested prior to field deployment. The same platform has been leveraged to develop a first of a kind reliability model with a sample size of ~10,000 lasers. The model indicates that temperature and optical power density are the relevant acceleration parameters for the failure mode, with a prediction of 0.09 FIT based on production baseline data containing ~55,800 lasers. The results are validated with a data set of ~6 million lasers shipped to customers participating in our 100% RMA/FA program, where a FIT of 0.05 has been determined. The results indicate that heterogeneously integrated lasers are well suited as a light source solution for CPO and other high-density laser arrays architectures.

ACKNOWLEDGEMENTS

We would like to acknowledge the multiple Intel co-workers and organizations that supported and enabled the results presented in this article. The work shared here is an effort of almost a decade, and we also would like to thank our former co-workers who were part of developing our reliability test platforms and reliability models. Finally, we would like to thank Dr. Robert Herrick for helpful discussion on laser reliability over the years.

REFERENCES

[1] A. V. Krishnamoorthy et al., “Progress in Low-Power Switched Optical Interconnects,” IEEE J. Sel. Top. Quantum Electron., vol. 17, no. 2, pp. 357–376, Mar. 2011, doi: 10.1109/JSTQE.2010.2081350A.

[2] L. Liao *et al*., "Silicon Photonics for Next-Generation Optical Connectivity," *2023 Optical Fiber Communications Conference and Exhibition (OFC)*, San Diego, CA, USA, 2023, pp. 1-3, doi: 10.1364/OFC.2023.Th3B.1.

[3] A. Gholami, Z. Yao, S. Kim, C. Hooper, M. W. Mahoney and K. Keutzer, "AI and Memory Wall," in *IEEE Micro*, vol. 44, no. 3, pp. 33-39, May-June 2024, doi: 10.1109/MM.2024.3373763.

[4] "AI Use Cases and Deployments Today, and Problem Statement for Future" - Bharath Muthiah, META; UCSB's Institute for Energy Efficiency - 2022 Emerging Technologies Review. [Online video]. Available at “https://www.uctv.tv/shows/AI-Use-Cases-and-Deployments-Today-and-Problem-Statement-for-Future-with-Bharath-Muthiah-38471”

[5] S. Fathololoumi *et al*., "Highly Integrated 4 Tbps Silicon Photonic IC for Compute Fabric Connectivity," *2022 IEEE Symposium on High-Performance Interconnects (HOTI)*, CA, USA, 2022, pp. 1-4, doi: 10.1109/HOTI55740.2022.00016.

[6] A. Bechtolsheim, “Large Scale AI Clusters: Network Architectures and Optics,” presented at the 2023 OCP Global Summit, San Jose, CA, USA: Open Compute Project, Oct. 2023. [Online]. Available: https://www.youtube.com/watch?v=emlZz-PbZH0&ab_channel=OpenComputeProject.

[7] L. A. Coldren, S. W. Corzine and M. L. Mashanovitch, [Diode Lasers and Photonic Integrated Circuits], USA:Wiley, New York, NY, , vol. 53, 2012.

[8] A. W. Fang, Hyundai Park, R. Jones, O. Cohen, M. J. Paniccia and J. E. Bowers, "A continuous-wave hybrid AlGaInAs-silicon evanescent laser," in IEEE Photonics Technology Letters, vol. 18, no. 10, pp. 1143-1145, May 2006, doi: 10.1109/LPT.2006.874690.

[9] JS-001-2024: Joint JEDEC/ESDA Standard For Electrostatic Discharge Sensitivity Test - Human Body Model (HBM) - Device Level.

[10] JESD22-C101E: Field-Induced Charged-Device Model Test Method for Electrostatic Discharge-Withstand Thresholds of Microelectronic Components.

[11] M. Fukuda and G. Iwane; “Degradation of active region in InGaAsP/InP buried heterostructure lasers,” *J. Appl. Phys.* 15 October 1985; 58 (8): 2932–2936. https://doi.org/10.1063/1.336298.

[12] O. Ueda and S. Tomiya, “Chapter 5 - Grown-in defects and thermal instability affecting the reliability of lasers: III–Vs versus III-nitrides,” in Reliability of Semiconductor Lasers and Optoelectronic Devices, R. W. Herrick and O. Ueda, Eds., in Woodhead Publishing Series in Electronic and Optical Materials, Woodhead Publishing, 2021, pp. 177–238. doi:10.1016/B978-0-12-819254-2.00004-7.

[13] I. Yonenaga. Mechanical Properties and Dislocation Dynamics in III-V Compounds. Journal de Physique III, 1997, 7 (7), pp.1435-1450. ff10.1051/jp3:1997198ff. ffjpa-00249656.

[14] R. W. Herrick, “Chapter 2 - Reliability engineering in optoelectronic devices and fiber optic transceivers,” in Reliability of Semiconductor Lasers and Optoelectronic Devices, R. W. Herrick and O. Ueda, Eds., in Woodhead Publishing Series in Electronic and Optical Materials, Woodhead Publishing, 2021, pp. 47–87. doi: 10.1016/B978-0-12-819254-2.00003-5.

[15] “GR-468 - Reliability Optoelectronic Devices Used | Telcordia.”

[16] C. H. Henry, P. M. Petroff, R. A. Logan, F. R. Merritt; Catastrophic damage of AlxGa$_{1-x}$As double-heterostructure laser material. *J. Appl. Phys.* 1 May 1979; 50 (5): 3721–3732. https://doi.org/10.1063/1.326278.

[17] A. Moser; Thermodynamics of facet damage in cleaved AlGaAs lasers. *Appl. Phys. Lett.* 29 July 1991; 59 (5): 522–524. https://doi.org/10.1063/1.105426.

[18] J. W. Tomm, M. Ziegler, M. Hempel, and T. Elsaesser, “Mechanisms and fast kinetics of the catastrophic optical damage (COD) in GaAs-based diode lasers,” Laser Photonics Rev. 5(3), 422–441 (2011). https://doi.org/10.1002/lpor.201000023.

[19] M. Belt, et. Al., "Sidewall gratings in ultra-low-loss Si3N4 planar waveguides," Opt. Express 21, 1181-1188 (2013). https://doi.org/10.1364/OE.21.001181.

[20] A. Barkai *et al*., "Double-Stage Taper for Coupling Between SOI Waveguides and Single-Mode Fiber," in *Journal of Lightwave Technology*, vol. 26, no. 24, pp. 3860-3865, Dec.15, 2008, doi: 10.1109/JLT.2008.928199.

[21] Y. Sin, N. Presser, B. Foran, N. Ives, S. C. Moss, "Catastrophic facet and bulk degradation in high power multi-mode InGaAs strained quantum well single emitters," Proc. SPIE 7198, High-Power Diode Laser Technology and Applications VII, 719818 (23 February 2009); https://doi.org/10.1117/12.807359.

[22] R. W. Herrick, C. B. Roxlo, T. H. O. Sjolund, and T. Sudo, “Methods for testing lasers using optical burn-in,” US8067949B2, Nov. 29, 2011.
[23] K. Häusler, A. Bawamia, J. Boschker, J. Baumann, M. Dammasch, H. Wenzel, A. Knigge, J. Fricke, A. Maassdorf, A. Wicht, "Operational lifetime qualification of laser diodes for BECCAL," Proc. SPIE 12777, International Conference on Space Optics — ICSO 2022, 1277746 (12 July 2023); https://doi.org/10.1117/12.2690674.
[24] 8.3.1.4. Accelerated life tests in NIST/SEMATECH e-Handbook of Statistical Methods; https://doi.org/10.18434/M32189
[25] A. Moser, E. E. Latta; Arrhenius parameters for the rate process leading to catastrophic damage of AlGaAs-GaAs laser facets. J. Appl. Phys. 15 May 1992; 71 (10): 4848–4853. https://doi.org/10.1063/1.350628